Journal of Power Sources 223 (2013) 30–35

Contents lists available at SciVerse ScienceDirect

Journal of Power Sources

journal homepage: www.elsevier.com/locate/jpowsour

Probing carbon edge exposure of iron phthalocyanine-based oxygen reduction catalysts by soft X-ray absorption spectroscopy

Hideharu Niwa [a], Makoto Saito [a], Masaki Kobayashi [a,b], Yoshihisa Harada [a,b], Masaharu Oshima [a,b,*], Shogo Moriya [c], Katsuyuki Matsubayashi [c], Yuta Nabae [c], Shigeki Kuroki [c], Takashi Ikeda [d], Kiyoyuki Terakura [e], Jun-ichi Ozaki [c,f], Seizo Miyata [c,g]

[a] Department of Applied Chemistry, School of Engineering, The University of Tokyo, 7-3-1 Hongo, Bunkyo-ku, Tokyo 113-8656, Japan
[b] Synchrotron Radiation Research Organization, The University of Tokyo, 7-3-1 Hongo, Bunkyo-ku, Tokyo 113-8656, Japan
[c] Department of Organic and Polymeric Materials, Graduate School of Science and Engineering, Tokyo Institute of Technology, 2-12-1 S8-26 Ookayama, Meguro-ku, Tokyo 152-8552, Japan
[d] Quantum Beam Science Directorate, Japan Atomic Energy Agency (JAEA), SPring-8, 1-1-1 Kouto, Sayo-cho, Sayo-gun, Hyogo 679-5148, Japan
[e] Research Center for Integrated Science, Japan Advanced Institute of Science Technology (JAIST), 1-1 Asahidai, Nomi, Ishikawa 923-1292, Japan
[f] Department of Chemical & Environmental Engineering, Graduate School of Engineering, Gunma University, 1-5-1 Tenjin-cho, Kiryu, Gunma 376-8515, Japan
[g] New Energy and Industrial Technology Development Organization, 1310 Omiya-cho, Saiwai-ku, Kawasaki, Kanagawa 212-8554, Japan

HIGHLIGHTS

- O_2 reduction site of FePc-based catalysts was characterized by C 1*s* X-ray absorption.
- Low energy shoulder of the π^* peak becomes a good indicator of active edge carbons.
- The method can be applied to characterize a wide variety of carbon-based catalysts.

ARTICLE INFO

Article history:
Received 28 July 2012
Received in revised form
8 September 2012
Accepted 12 September 2012
Available online 18 September 2012

Keywords:
Polymer electrolyte fuel cell
Cathode
Oxygen reduction reaction
X-ray absorption spectroscopy
Carbon-based catalysts
Electronic structure

ABSTRACT

Recently carbon-based catalysts have attracted much attention for its high ability to catalyze oxygen reduction reaction (ORR) in a cathode for polymer electrolyte fuel cells. Among active site models of the catalyst, edge region of sp^2 carbon network is expected to demonstrate high ORR activity comparable to platinum catalysts. However, it is difficult to directly identify the chemical structure of the edge sites by applying conventional structural or electronic probes to actual catalysts. Here, we used C 1*s* X-ray absorption spectroscopy to observe electronic structure of carbon in iron phthalocyanine-based catalysts, and found a signature of edge exposure below the π^* edge, whose intensity is well correlated with the ORR activity. Combined with information about the chemical structure of nitrogen, ORR activity of the catalyst is characterized in terms of the edge exposure.

1. Introduction

Polymer electrolyte fuel cells (PEFCs) have attracted much attention as clean and high efficient electrochemical devices for energy conversion [1]. Conventionally, Pt-based materials are used as cathode catalysts for slow oxygen reduction reaction (ORR). Alternative ORR catalysts of low cost and high activity are desired because Pt is expensive and their resources are limited. Carbon-based materials are expected to be cathode catalysts alternative to conventional Pt catalysts for PEFCs [2–4]. Carbon-based catalysts are usually synthesized by pyrolyzing precursors such as metal-phthalocyanine or metal-porphyrin with/without other carbon resources such as resins to improve ORR activities [5–18]. Accordingly, carbon-based catalysts are generally composed of C, N, O, H,

* Corresponding author. Department of Applied Chemistry, School of Engineering, The University of Tokyo, 7-3-1 Hongo, Bunkyo-ku, Tokyo 113-8656, Japan. Tel.: +81 3 5841 7191; fax: +81 3 5841 8744.
E-mail address: oshima@sr.t.u-tokyo.ac.jp (M. Oshima).

0378-7753/$ – see front matter © 2012 Elsevier B.V. All rights reserved.
http://dx.doi.org/10.1016/j.jpowsour.2012.09.031

and 3*d* transition metals. It is crucial for development of PEFC whether or not the ORR activity of carbon-based catalysts doped with light elements and/or non-precious metals could surpass the ability of Pt-based catalysts. Thus, elucidation of ORR active sites is strongly required for further improving the ORR activity of carbon-based catalysts.

The ORR active sites of carbon-based catalysts have long been ascribed to metal-N_x sites originated or derived from the macrocycle in its precursor [4–9]. On the other hand, recently it has been proposed that carbon and/or nitrogen sites are the ORR active sites in some sort of carbon-based catalysts [10–22]. For example, Matter et al. claimed that pyridinic-N, or pyridine-like N, detected by X-ray photoelectron spectroscopy (XPS) is an indicator for the edge plane because those nitrogen functionalities should exist at the edge plane and proposed that the edge plane is the active site for ORR [10]. Using first principles calculation, Ikeda et al. reported that carbon atoms located at the zigzag edge tend to adsorb oxygen molecule [19]. In addition, they suggested that when graphite-like nitrogen is doped at the zigzag edge, the oxygen adsorption and subsequent ORR activities of the neighboring zigzag edge carbon are enhanced. In previous experimental studies on metal phthalocyanine-based catalysts, we found that the high ORR active catalysts have relatively large proportion of graphite-like nitrogen and proposed a correlation between graphite-like nitrogen and the ORR activities [20–22]. Moreover, in this metal containing carbon-based materials, metals in the precursor are responsible for the formation of the ORR active carbon structure [23,24] while they do not work as the dominant ORR active site for carbon-based catalysts pyrolyzed at high temperatures [17]. On this account, it is necessary to identify the highly active edge carbon structures for ORR. However, to the best of our knowledge, direct evidence of such carbon sites has not been shown yet.

Experimentally, methods to directly identify the local configuration of carbon atoms at edges are limited. There are several reports on well-defined carbon materials such as graphene [25–27], while there are few reports on the electronic states for carbon edges of porous carbon materials including carbon-based catalysts. Raman spectroscopy and X-ray diffraction measurements can distinguish sp^2 graphitic components from defective components [12–16], while it is quite difficult to deduce the information of carbon edges. Transmission electron microscope (TEM) technique is a powerful tool to observe materials on an atomic scale. For instance, defective carbon edges at the surface of the carbon-based catalysts have been reported [10,14,16]. However, the electronic states of edge carbons of porous carbon materials are hardly detected even by TEM combined with EELS (electron energy loss spectroscopy) technique [27]. Although XPS is widely used in order to analyze chemical species in carbon-based catalysts [9–13,15,16,18], it would be difficult to directly obtain electronic and/or structural information of carbon edges by C 1*s* XPS because C 1*s* XPS spectra mainly consist of a structure-less asymmetric peak originated from sp^2 carbon and therefore the signal from carbon edges is indistinct.

In this paper, we used C 1*s* X-ray absorption spectroscopy (XAS) to investigate electronic properties related to the ORR activity of the catalysts. Fine structures in C 1*s* XAS spectra provide fruitful information about edge carbons as well as bulk sp^2/sp^3 carbon structures [28,29]. We have examined catalysts synthesized from iron phthalocyanine (FePc) mixed with phenolic resin (PhRs) because they are one of the most typical carbon-based catalysts having high ORR activity [30]. In order to identify the carbon structure that is responsible for the ORR activity, the electronic structure of carbon in the catalysts pyrolyzed at various temperatures has been analyzed by C 1*s* XAS.

2. Experimental

The samples were synthesized by pyrolyzing a mixture of FePc (Tokyo Kasei) and PhRs (Gunei Chemical, PSK-2320). PhRs was dissolved in acetone and then FePc was added under ultrasonication, where the amount of iron in the mixture was adjusted to be 3 wt.%. After removal of solvent with a rotary evaporator, the FePc/PhRs was pyrolyzed in an inert gas stream at various temperatures from 200 °C to 800 °C for 5 h. Here for example, Fe200 denotes the FePc-based catalysts pyrolyzed at 200 °C. Characterization of the FePc-based catalysts has been described elsewhere [17].

The ORR activity of the FePc-based catalysts was measured by rotating disk electrode (RDE) voltammetry using O_2-saturated 0.5 mol L^{-1} H_2SO_4 solution at room temperature. The catalyst ink was made by mixing the catalyst powder with Nafion solution (5 wt.% Aldrich), ethanol, and water. 0.2 mg cm^{-2} of the catalyst ink was loaded on the RDE and the linear sweep voltammetry (LSV) was measured with a rotating speed of 1500 rpm. The LSV for ORR was obtained by subtracting the data recorded under N_2-saturated H_2SO_4 solution from the data under O_2-saturated H_2SO_4 solution. The electrical conductivity of the FePc-based catalysts was measured with a resistivity meter (Mitsubishi Chemical, Loresta GP) applying a pressure of 4 MPa. C 1*s* XAS measurements were performed at soft X-ray beam line BL-7A of Photon Factory, KEK and BL27SU of SPring-8, Japan. The XAS spectra were recorded in the total electron yield mode by measuring the sample current and then normalized to the mirror current. The vacuum and temperature condition in the experiments were 2×10^{-8} Torr and room temperature. The energy calibration was performed using the Au $4f_{7/2}$ photoemission line taken to be 83.9 eV.

3. Results and discussion

Fig. 1 shows results on RDE measurements for the FePc-based catalysts [17]. The catalysts pyrolyzed above 550 °C show ORR activities. Fe600 shows the best catalytic activity for ORR among the FePc-based catalysts in this study. The electrical conductivity of the FePc-based catalysts is shown in Fig. 2. Between pyrolysis temperatures of 500 °C and 600 °C, the electrical conductivity is greatly improved by a factor of 10^7, which can be well correlated with the steep rise of the ORR activity around 600 °C.

Fig. 3 shows C 1*s* XAS spectra of the FePc-based catalysts pyrolyzed at various temperatures. In all the samples, the π* resonant peak originating from C 1*s* → π* excitation is observed at around

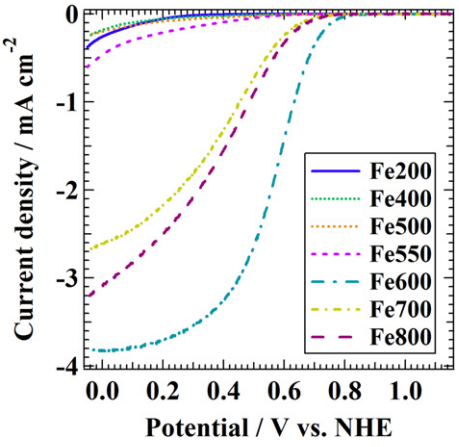

Fig. 1. Voltammograms of the FePc-based catalysts [17]. Current densities are normalized to the geometric electrode area.

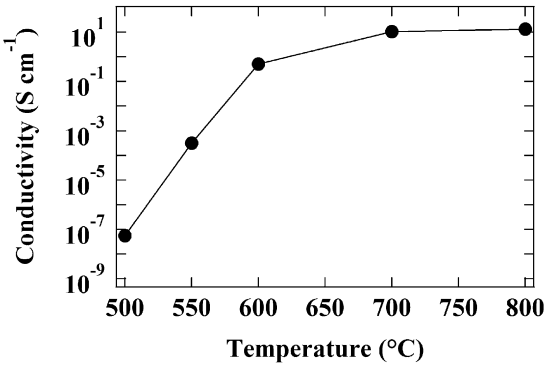

Fig. 2. Electrical conductivity of the FePc-based catalysts.

284.8 eV and the σ* resonant peak derived from C 1*s* → σ* excitation is observed at around 291.7 eV. In addition, at least four components (peaks A, B, C, and D) are observed in the spectra. The profiles of the C 1*s* XAS spectra change systematically with pyrolyzing temperature. The spectral profile of Fe200 sample is quite similar to that of the mixture of FePc and PhRs (FePc/PhRs) precursors. Although the profiles of B and C are similar to those of FePc, a shoulder peak at around 284 eV observed in FePc disappears in Fe200, suggesting that PhRs and a part of FePc seem to be decomposed already at 200 °C. Fe400 has a broader π* peak than Fe200 and profiles of the peaks B and C have changed, indicating that both PhRs and FePc components are drastically decomposed at 400 °C. The most active catalyst Fe600 shows unique C 1*s* XAS profile among all the samples; a shoulder peak A appears at 1.2 eV below the π* resonant peak and a prominent peak C emerges between π* and σ* resonant peaks. Note that Fe550 and Fe600 have similar peak profiles of the C 1*s* XAS spectra while their ORR activities are quite different partly due to 1000 times larger electrical conductivity of Fe600 than that of Fe550. The improved electrical conductivity of Fe600 is probably originated from the growth of sp^2 graphitic structure which is sufficient for electronic

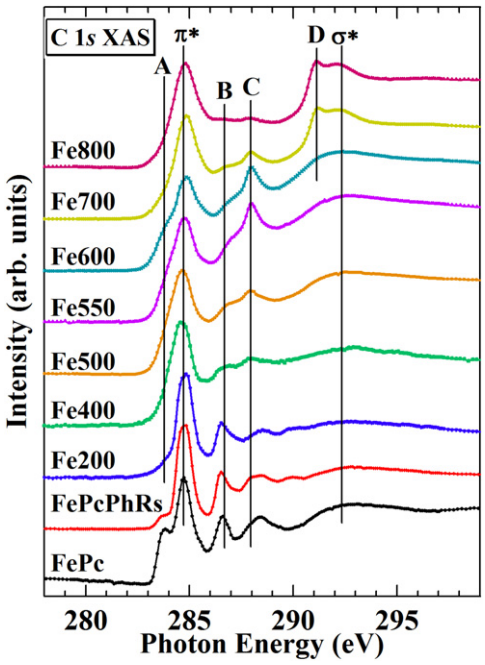

Fig. 3. C 1*s* XAS spectra of the FePc-based catalysts.

conduction along the basal plane of the samples. The electrical conductivity up to 0.5 S cm^{-1} in Fe600 is even higher than the proton conductivity of 0.1 S cm^{-1} for conventional Nafion membrane. However, this is not clearly reflected on the C 1*s* XAS spectra. On the other hand, the samples pyrolyzed at higher temperatures (Fe700 and Fe800) show an indicator of highly developed conductive graphitic structure as a σ* exciton peak D at 291 eV in the XAS spectra, which can be well correlated with a much improved electrical conductivity of them [31,32]. The improved electrical conductivity no longer contributes to the increase of the ORR activity possibly because the conductivity already improves sufficiently at pyrolysis temperature of 600 °C while the ORR active sites decreases due to desorption or incorporation into bulk during the growth of sp^2 graphitic structure.

In order to clarify the origin of each component, the C 1*s* XAS spectra are decomposed by using Gauss functions as peak components. Within the framework of the simplest free-electron approximation, two step functions broadened by the Gaussian are considered as backgrounds, which are transitions to the continuum of π* and σ* states. Each width is an adjustable parameter considering a broadening due to inhomogeneity of the samples. This analysis is similar to those performed by Batson [33], Jiménez et al. [34], and Medjo et al. [35]. Fig. 4(a)–(f) shows results for the peak decomposition of the C 1*s* XAS spectra of the FePc-based catalysts (Fe400, Fe500, Fe550, Fe600, Fe700 and Fe800). Since sp^2 carbon is the main component of the FePc-based catalysts, relative number of each carbon component can be estimated from the intensity ratio of each decomposed peak to the π* peak. Fig. 5 shows a relation between the intensity ratio and oxygen reduction current density at 0.6 V vs. NHE which seems unaffected by oxygen diffusion. Since the current density is determined by the absolute amount of active sites in a unit area, one might assume that the difference in specific surface area of the catalyst is responsible for the ORR current. However, as demonstrated in Fig. 6, when the current densities at 0.6 V are normalized by the BET surface area [17], the normalized current densities as a function of pyrolysis temperature show the same tendency as those normalized to the geometric electrode area. As shown in Fig. 5(a), the intensity ratio of the peak A to the π* peak (A/π*) and current densities at 0.6 V vs. NHE show similar tendencies as a function of pyrolysis temperature of the catalysts, which indicates a correlation between the peak A component and the ORR activity.

Ozaki et al. speculated that the ORR activity originated from edge sites of graphite structure from TEM observation [16] and XRD coupled with the Diamond analysis [36]. So, the most possible origin for the peak A should be edge sites. One possibility is the edge states in graphene [26,37]. Typically, carbon in graphene has two types of edges, namely armchair edge and zigzag edge [37]. The density of states (DOS) near the Fermi level of these two types of edges are quite different. The armchair edge does not modify the basic electronic structure of bulk graphite near the Fermi level, while the zigzag edge has sharp DOS at the Fermi level along with bulk π and π* bands [37]. Entani et al. have reported the observation of a shoulder structure at lower energy side of the π* peak in C 1*s* XAS of nanographene, which they attributed to the empty state near the Fermi level characteristic to the zigzag edge state [26]. The energy difference between the shoulder structure and the π* peak in the nanographene is 1.3 eV, which coincides well with the peak A in our present results. However, this assignment has been challenged by a recent theoretical analysis of C 1*s* XAS by Hou et al. [29]. According to their analysis, the large DOS of the edge states close to the Fermi level can screen the attractive potential created by the C 1*s* core hole, leading to a smaller C 1*s* binding energy. Due to this screening effect, the XAS peak associated with the transition to the zigzag edge states will be located at 2.5 eV below the π* peak.

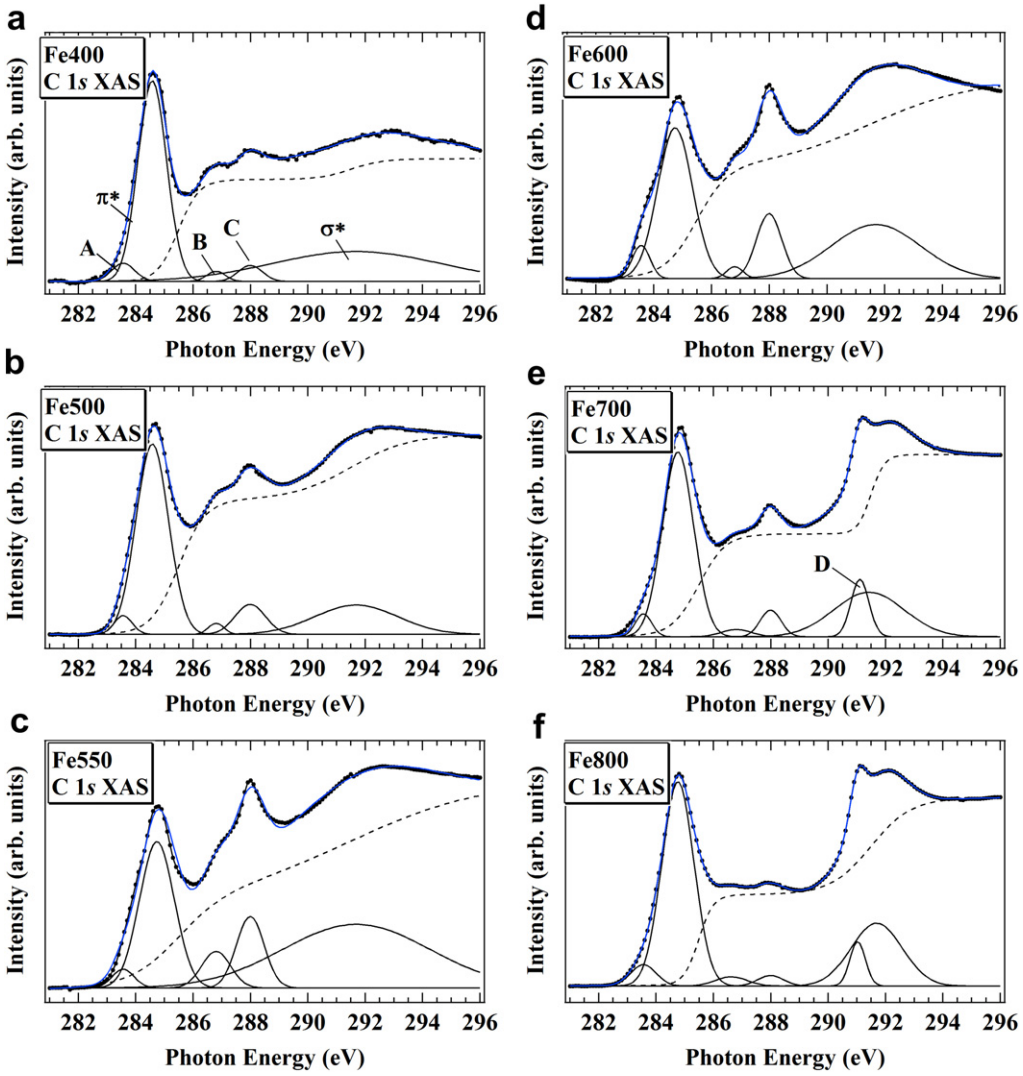

Fig. 4. Decomposed C 1*s* XAS spectra of (a) Fe400, (b) Fe500, (c) Fe550, (d) Fe600, (e) Fe700, and (f) Fe800. Dotted lines are the measured data, blue solid lines are fitted curve, black solid lines are decomposed peak components, and dashed lines are backgrounds. (For interpretation of the references to colour in this figure legend, the reader is referred to the web version of this article.)

Moreover, monohydrogenated zigzag edge is energetically unstable except under very low hydrogen pressure, thus the termination of the zigzag edge may be a mixture of monohydrogenation and dihydrogenation [38]. Examples of such carbon structures are shown in Fig. 7. It has been demonstrated that the shoulder structure around 1.3 eV below the π^* peak and the peak A in our results for the FePc-based catalysts can be reproduced in such a situation. Both a monohydrogenated zigzag edge carbon next to a dihydrogenated zigzag edge carbon indicated by the symbol in Fig. 7(a) and a zigzag edge-1 carbon next to a dihydrogenated zigzag edge carbon indicated by the symbol in Fig. 7(b) can contribute to the peak A [29]. Therefore, Fig. 5(a) directly indicates that there is a relationship between the edge carbon exposure and the ORR activity.

Although the intensity of the peak C at 288.0 eV also seems to be enhanced for the highly ORR active Fe600 catalyst, Fig. 5(c) does not show an apparent correlation between the intensity of the peak C and the ORR activity. Close to the peak C, Entani et al. have assigned a peak at 287.5 eV to C—H σ^* bond [26] and Hou et al. have found that the peaks at 287 and 288 eV originate from the resonances of the σ^* states of sp^2 hybridized C—H and sp^3 hybridized C—H_2 both at zigzag and armchair edges, respectively [29]. If the peak C originates only from the edge carbons assigned above, the intensity of the peak C might show a correlation with the ORR activity. However, the absence of apparent correlation in Fig. 5(c) implies contribution of functional moieties other than the edge carbons to the peak C. It has been reported that when carbon materials contain oxygen, oxygen-containing functional groups produce the peak in this energy region [39,40]. Moreover, a peak due to nitrogen–carbon bonds appears in this region in the case of nitrogen-doped carbon materials [32]. In fact, Fe550, which has the largest intensity of the peak C, contains more nitrogen than Fe600 [17]. Although the 1000 times lower electrical conductivity of Fe550 than that of Fe600 predominates the ORR profile which lacks an apparent correlation with the peak C intensity, it is possible that the nitrogen–carbon bonds responsible for the peak C constitutes the ORR active site. Fig. 5(b) shows that there is no correlation between the intensity of the peak B and the ORR activity.

Previous studies on XAS and XPS analyses of metal phthalocyanine-based catalysts showed that highly ORR active catalysts contain relatively high amount of graphite-like nitrogen [20,21]. During the synthesis of the FePc-based catalysts, graphite-like nitrogen starts to be formed at around 600 °C [22]. This coincides with the temperature where the relative peak intensity of the peak A

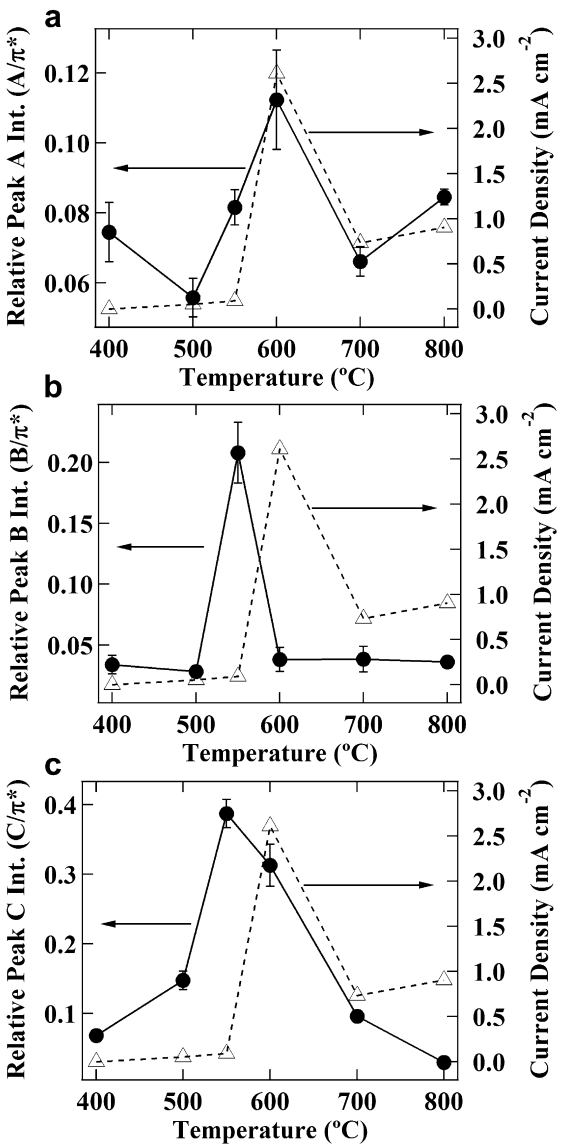

Fig. 5. Intensity ratio of each peaks to the π^* peak (solid circle line) and current densities at 0.6 V vs. NHE (dashed triangle line) compared with pyrolysis temperature of the catalysts. (a) Relative peak intensity of the peak A to the π^* peak (A/π^*), (b) relative peak intensity of the peak B to the π^* peak (B/π^*), and (c) relative peak intensity of the peak C to the π^* peak (C/π^*).

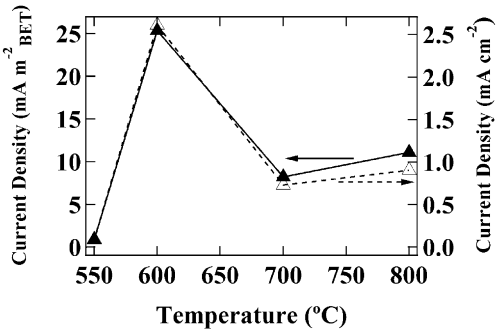

Fig. 6. Current densities at 0.6 V vs. NHE normalized by the BET surface area (solid triangle line; left axis) and current densities at 0.6 V derived from a geometric surface area of the carbon disk electrode (dashed triangle line; right axis) compared with pyrolysis temperature of the FePc-based catalysts.

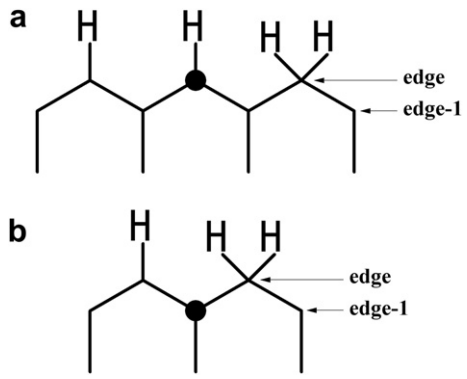

Fig. 7. The example of carbon edges with (a) monohydrogenated zigzag edge carbon neighboring a monohydrogenated carbon and a dihydrogenated carbon and (b) zigzag edge-1 carbon next to two dihydrogenated zigzag edge carbon. The referred carbon atoms are indicated by the symbol (circle). Other examples and their peak positions are described elsewhere [29].

to the π^* peak is most enhanced and the intensity of the peak C, a part of which can be originated from nitrogen–carbon bonds, is also prominent. Considering the present results along with the previous studies, it is suggested that the ORR active sites of the FePc-based catalysts include graphite-like nitrogen existing at edge sites.

4. Conclusions

In conclusion, electronic structure of carbon in the FePc-based samples pyrolyzed at various temperatures was directly investigated by XAS and correlation between the electronic structure and the ORR activity was found. The shoulder peak A (at around 283.6 eV) of the π^* resonant C 1*s* peak can be attributed to monohydrogenated zigzag edge carbon and zigzag edge-1 carbons both being next to dihydrogenated zigzag edge carbon. The intensity of the peak A corresponding to the edge carbons described above has a correlation with the ORR activity. Therefore, the peak A at around 283.6 eV, which is a good indicator of the edge sites, can be used for optimizing the fabrication processes of the carbon-based oxygen reduction catalysts with improved ORR activity. It is also possible that some components of the peak C at 288.0 eV between the π^* and σ^* resonant peak constitute ORR active sites, although an apparent relationship between the ORR activity and the peak at 288.0 eV was not observed due to a stark difference in electrical conductivity. A detailed study on the correlation between the peak A and graphite-like nitrogen next to the edge carbon will be done in the near future.

Acknowledgment

This work was performed under Project 08003440-0 at the New Energy and Industrial Technology Development Organization (NEDO). The authors thank K. Amemiya and R. Sumii for their technical supports during XAS measurements at the Photon Factory and T. Muro, Y. Tamenori and Y. Kato at SPring-8. This work has been performed under the approval of the Photon Factory Program Advisory Committee (Proposal No. 2008G678) and under the approval of the Japan Synchrotron Radiation Research Institute (JASRI) (Proposal No. 2008B1177, and 2009A1008).

References

[1] P. Costamagna, S. Srinivasan, J. Power Sources 102 (2001) 242–252.
[2] G. Liu, X. Li, J.-W. Lee, B.N. Popov, Catal. Sci. Technol. 1 (2011) 207.
[3] D. Yu, E. Nagelli, F. Du, L. Dai, J. Phys. Chem. Lett. 1 (2010) 2165–2173.
[4] F. Jaouen, E. Proietti, M. Lefèvre, R. Chenitz, J.-P. Dodelet, G. Wu, H.T. Chung, C.M. Johnston, P. Zelenay, Energy Environ. Sci. 4 (2011) 114–130.

[5] G. Wu, K.L. More, C.M. Johnston, P. Zelenay, Science 332 (2011) 443–447.
[6] M. Lefèvre, E. Proietti, F. Jaouen, J.-P. Dodelet, Science 324 (2009) 71–74.
[7] D. Nguyen-Thanh, A.I. Frenkel, J. Wang, S. O'Brien, D.L. Akins, Appl. Catal. B Environ. 105 (2011) 50–60.
[8] S. Pylypenko, S. Mukherjee, T. Olson, P. Atanassov, Electrochim. Acta 53 (2008) 7875–7883.
[9] U.I. Kramm, I. Abs-Wurmbach, I. Herrmann-Geppert, J. Radnik, S. Fiechter, P. Bogdanoff, J. Electrochem. Soc. 158 (2011) B69–B78.
[10] P. Matter, L. Zhang, U. Ozkan, J. Catal. 239 (2006) 83–96.
[11] J.Y. Choi, R.S. Hsu, Z. Chen, J. Phys. Chem. C 114 (2010) 8048–8053.
[12] Z. Luo, S. Lim, Z. Tian, J. Shang, L. Lai, B. MacDonald, C. Fu, Z. Shen, T. Yu, J. Lin, J. Mater. Chem. 21 (2011) 8038–8044.
[13] M. Chisaka, T. Iijima, A. Tomita, T. Yaguchi, Y. Sakurai, J. Electrochem. Soc. 157 (2010) B1701–B1706.
[14] R. Liu, D. Wu, X. Feng, K. Müllen, Angew. Chem. Int. Ed. 49 (2010) 2565–2569.
[15] C.V. Rao, C.R. Cabrera, Y. Ishikawa, J. Phys. Chem. Lett. 1 (2010) 2622–2627.
[16] J. Ozaki, S. Tanifuji, A. Furuichi, K. Yabutsuka, Electrochim. Acta 55 (2010) 1864–1871.
[17] Y. Nabae, M. Malon, S.M. Lyth, S. Moriya, K. Matsubayashi, N. Islam, S. Kuroki, M. Kakimoto, J. Ozaki, S. Miyata, ECS Trans. (2009) 463–467.
[18] G. Liu, X. Li, P. Ganesan, B.N. Popov, Electrochim. Acta 55 (2010) 2853–2858.
[19] T. Ikeda, M. Boero, S. Huang, K. Terakura, M. Oshima, J. Ozaki, J. Phys. Chem. C 112 (2008) 14706–14709.
[20] H. Niwa, K. Horiba, Y. Harada, M. Oshima, T. Ikeda, K. Terakura, J.-ichi Ozaki, S. Miyata, J. Power Sources 187 (2009) 93–97.
[21] H. Niwa, M. Kobayashi, K. Horiba, Y. Harada, M. Oshima, K. Terakura, T. Ikeda, Y. Koshigoe, J.-ichi Ozaki, S. Miyata, S. Ueda, Y. Yamashita, H. Yoshikawa, K. Kobayashi, J. Power Sources 196 (2011) 1006–1011.
[22] Y. Harada, M. Kobayashi, H. Niwa, M. Saito, M. Oshima, Hyomen Kagaku 32 (2011) 716–722 (in Japanese).
[23] K. Wiesener, Electrochim. Acta 31 (1986) 1073–1078.
[24] M. Kobayashi, H. Niwa, M. Saito, Y. Harada, M. Oshima, H. Ofuchi, K. Terakura, T. Ikeda, Y. Koshigoe, J.-ichi Ozaki, S. Miyata, Electrochim. Acta 74 (2012) 254–259.
[25] K. Suenaga, M. Koshino, Nature 468 (2010) 1088–1090.
[26] S. Entani, S. Ikeda, M. Kiguchi, K. Saiki, G. Yoshikawa, I. Nakai, H. Kondoh, T. Ohta, Appl. Phys. Lett. 88 (2006) 153126.
[27] Z. Liu, K. Suenaga, P. Harris, S. Iijima, Phys. Rev. Lett. 102 (2009) 1–4.
[28] J. Stöhr, NEXAFS Spectroscopy, Springer, Berlin, Germany, 1992.
[29] Z. Hou, X. Wang, T. Ikeda, S.-feng Huang, K. Terakura, M. Boero, M. Oshima, M.-aki Kakimoto, S. Miyata, J. Phys. Chem. C 115 (2011) 5392–5403.
[30] R. Jasinski, J. Electrochem. Soc. 112 (1965) 526–528.
[31] Y. Ma, P. Skytt, N. Wassdahl, P. Glans, J. Guo, J. Nordgren, Phys. Rev. Lett. 71 (1993) 3725–3728.
[32] N. Hellgren, J. Guo, Y. Luo, C. Såthe, A. Agui, S. Kashtanov, J. Nordgren, H. Ågren, J.-E. Sundgren, Thin Solid Films 471 (2005) 19–34.
[33] P. Batson, Phys. Rev. B 48 (1993) 2608–2610.
[34] I. Jiménez, R. Gago, J.M. Albella, Diamond Relat. Mater. 12 (2003) 110–115.
[35] R.E. Medjo, B.T. Sendja, J.M. Mane, P.O. Ateba, Phys. Scr. 80 (2009) 055602.
[36] J. Ozaki, N. Kimura, T. Anahara, A. Oya, Carbon 45 (2007) 1847–1853.
[37] M. Fujita, K. Wakabayashi, K. Nakada, K. Kusakabe, J. Phys. Soc. Jpn. 65 (1996) 1920–1923.
[38] T. Wassmann, A. Seitsonen, A. Saitta, M. Lazzeri, F. Mauri, Phys. Rev. Lett. 101 (2008) 096402.
[39] R. Larciprete, S. Gardonio, L. Petaccia, S. Lizzit, Carbon 47 (2009) 2579–2589.
[40] V.a Coleman, R. Knut, O. Karis, H. Grennberg, U. Jansson, R. Quinlan, B.C. Holloway, B. Sanyal, O. Eriksson, J. Phys. D Appl. Phys. 41 (2008) 062001.